

$B\bar{B}$ angular correlations at the LHC in parton Reggeization approach merged with higher-order matrix elements

A.V.Karpishkov,^{*} M.A. Nefedov,[†] and V.A.Saleev[‡]

Samara National Research University,

Moscow Highway, 34, 443086, Samara, Russia

Abstract

We calculate the angular distribution spectra between beauty (B) and anti-beauty (\bar{B}) mesons in proton-proton collisions in the leading order approximation of the parton Reggeization approach consistently merged with the next-to-leading order corrections from the emission of additional hard gluon. To describe b-quark hadronization we use the universal scale-depended parton-to-meson fragmentation functions extracted from the world e^+e^- annihilation data. We have obtained good agreement between our predictions and data from the CMS Collaboration at the energy $\sqrt{S} = 7$ TeV for $B\bar{B}$ angular correlations within uncertainties and without free parameters. Predictions for analogous correlation observables at $\sqrt{S} = 13$ TeV are provided.

PACS numbers: 12.38.-t, 12.40.Nn, 13.85.Ni, 14.40.Lb

^{*}Electronic address: karpishkov@rambler.ru

[†]Electronic address: nefedovma@gmail.com

[‡]Electronic address: saleev@samsu.ru

I. INTRODUCTION

Production of b -quarks in the high energy pp -collisions is the object of an intensive experimental study at the CERN LHC. In the present paper we focus on a measurements of $b\bar{b}$ angular and momentum correlations, since they provide a test of dynamics of hard interactions, which is highly sensitive to the higher-order corrections in QCD. There are two ways of study these $b\bar{b}$ correlations. The first one is based on reconstruction of pairs of b -jets [1, 2], in the second case we get information on dynamics of hard production of $b\bar{b}$ -pair using data on pair production of B -mesons. In turn, long-lived B -mesons are reconstructed via their semileptonic decays. One advantage of the latter method is the unique capability to detect $B\bar{B}$ -pairs even at small opening angles, in which case the decay products of the B -hadrons tend to be merged into a single jet and the standard b -jet tagging techniques are not applicable [3].

On the theory side, one has to take into account multiple radiation of both soft/collinear and hard additional partons to describe such angular correlations over the whole observable range of opening angles between momenta of B -mesons. In the Leading Order (LO) of Collinear Parton Model (CPM), b -quarks are produced back-to-back in azimuthal angle. Effects of the soft and collinear Initial State Radiation (ISR) or Final State Radiation (FSR) somewhat smear the distribution in azimuthal angle difference between transverse momenta of mesons ($\Delta\phi$) around $\Delta\phi \simeq \pi$. These effects are systematically taken into account with the Leading Logarithmic Accuracy in the Parton Showers (PS) of the standad Monte-Carlo (MC) generators, such as PYTHIA or HERWIG.

Radiation of the additional hard gluons or quarks cause B and \bar{B} mesons to fly with $\Delta\phi < \pi$, but such radiation is beyond the formal accuracy of standard PS. Description of such events essentially depends on the way, how transverse momentum and the “small” light-cone component of momentum of the emitted parton are dealt with inside a PS algorithm, so called *recoiling scheme* [4]. Usually the accuracy of description of such kinematic configurations is improved via different methods of *matching* of the full NLO corrections in CPM with the parton-shower, such as MC@NLO [5] or POWHEG [6] or via *merging* of the kinematically and dynamically accurate description of a few additional hard emissions, provided by the exact tree-level matrix elements, with the soft/collinear emissions from the PS [7].

The presence of additional free parameters in the matching/merging methods, as well as the multitude of possible recoiling schemes, clearly calls for the improved understanding of the high- p_T regime of the PS from the point of view of Quantum Field Theory. Apart from the soft and collinear limits, the only known limit of scattering amplitudes in QCD which structure is sufficiently simple for the theoretical analysis is the limit of Multi-Regge kinematics (MRK), when emitted partons are highly separated in rapidity from each-other. This makes the MRK-limit to be a natural starting point for the construction of improved approximations. In the present paper, we construct the factorization formula and the framework of LO calculations in the Parton Reggeization Approach (PRA), which unifies the PS-like description of the soft and collinear emissions with the MRK limit for hard emissions. Then we switch to the description of the angular correlations in the production of $B\bar{B}$ -pairs accompanied by the hard jet, which sets the scale of the process. The present study is motivated by experimental data of the Ref. [3], since neither MC-calculations in the experimental paper, nor the calculations in the LO of k_T -factorization approach in the Ref. [8] could accurately describe the shape of angular distributions. We construct the consistent prescription, which *merges* the LO PRA calculation for this process with tree-level NLO matrix element. The latter improves description of those events, in which not the b -jet, but the hard gluon jet is the leading one, while avoiding possible double-counting and divergence problems. In such a way we achieve a good description of the shape of all $B\bar{B}$ correlation spectra without additional free parameters.

The paper has following structure. We describe the basics of PRA and it's relationships with other approaches in the Sec. II. In the Sec. III we present our merging prescription and the analytic and numerical tools, which we use. Then we concentrate on the numerical results, comparison with experimental data of the Ref. [3] and predictions for possible future measurements in the Sec. IV. Finally, we summarize our conclusions in the Sec. V.

II. LO PRA FRAMEWORK

To derive the factorization formula of the PRA in LO approximation, let us consider production of the partonic final state of interest \mathcal{Y} in the following auxilliary hard subprocess:

$$g(p_1) + g(p_2) \rightarrow g(k_1) + \mathcal{Y}(P_A) + g(k_2), \quad (1)$$

where the four-momenta of particles are denoted in parthenses, and $p_1^2 = p_2^2 = k_1^2 = k_2^2 = 0$. The final state \mathcal{Y} sets the hard scale μ^2 of the whole process via it's invariant mass $M_{\mathcal{A}}^2 = P_{\mathcal{A}}^2$, or transverse momentum $P_{T\mathcal{A}}$, otherwise it can be arbitrary combination of QCD partons. In a frame, where $\mathbf{p}_1 = -\mathbf{p}_2$ directed along the Z-axis it is natural to work with the Sudakov(light-cone) components of any four-momentum k :

$$k^\mu = \frac{1}{2} \left(k^+ n_-^\mu + k^- n_+^\mu \right) + k_T^\mu,$$

where $n_\pm^\mu = (n^\pm)^\mu = (1, 0, 0, \mp 1)^\mu$, $n_\pm^2 = 0$, $n_+ n_- = 2$, $k^\pm = k_\pm = (n_\pm k) = k^0 \pm k^3$, $n_\pm k_T = 0$, so that $p_1^- = p_2^+ = 0$ and $s = (p_1 + p_2)^2 = p_1^+ p_2^- > 0$. The dot-product of two four-vectors k and q in this notation is equal to:

$$(kq) = \frac{1}{2} \left(k^+ q_- + k^- q_+ \right) - \mathbf{k}_T \mathbf{q}_T.$$

For the discussion of different kinematic limits of the process (1) it is convinient to introduce the “ t -channel” momentum transfers $q_{1,2} = p_{1,2} - k_{1,2}$, which implies that $\mathbf{q}_{T1,2} = -\mathbf{k}_{T1,2}$, $q_1^- = -k_1^-$ and $q_2^+ = -k_2^+$. Let us define $t_{1,2} = \mathbf{q}_{T1,2}^2$, and the corresponding fractions of the “large” light-cone components of momenta:

$$z_1 = \frac{q_1^+}{p_1^+}, \quad z_2 = \frac{q_2^-}{p_2^-},$$

for the further use. Variables $z_{1,2}$ satisfy the conditions $0 \leq z_{1,2} \leq 1$ because $k_{1,2}^\pm \geq 0$ and $q_1^+ = P_{\mathcal{A}}^+ + k_2^+ \geq 0$, $q_2^- = P_{\mathcal{A}}^- + k_1^- \geq 0$ since all final-state particles are on-shell.

In the *collinear limit* (CL), when $\mathbf{k}_{T1,2}^2 \ll \mu^2$, while $0 \leq z_{1,2} \leq 1$, the asymptotic for the square of tree-level matrix element for the subprocess (1) is very well known:

$$|\overline{\mathcal{M}}|_{\text{CL}}^2 \simeq \frac{4g_s^4}{\mathbf{k}_{T1}^2 \mathbf{k}_{T2}^2} P_{gg}(z_1) P_{gg}(z_2) \frac{|\overline{\mathcal{A}_{CPM}}|^2}{z_1 z_2}, \quad (2)$$

where the bar denotes averaging (summation) over the spin and color quantum numbers of the initial(final)-state partons, $g_s = \sqrt{4\pi\alpha_s}$ is the coupling constant of QCD, $P_{gg}(z) = 2C_A ((1-z)/z + z/(1-z) + z(1-z))$ is the LO gluon-gluon DGLAP splitting function and \mathcal{A}_{CPM} is the amplitude of the subprocess $g(z_1 p_1) + g(z_2 p_2) \rightarrow \mathcal{Y}(P_{\mathcal{A}})$ with on-shell initial-state gluons. The error of approximation (2) is suppressed as $O(\mathbf{k}_{T1,2}^2/\mu^2)$ w. r. t. the leading term.

The limit of *Multi-Regge Kinematics* (MRK) for the subprocess (1) is defined as:

$$\Delta y_1 = y(k_1) - y(P_{\mathcal{A}}) \gg 1, \quad \Delta y_2 = y(P_{\mathcal{A}}) - y(k_2) \gg 1, \quad (3)$$

$$\mathbf{k}_{T1}^2 \sim \mathbf{k}_{T2}^2 \sim M_{T\mathcal{A}}^2 \sim \mu^2 \ll s, \quad (4)$$

where rapidity for the four-momentum k is equal to $y(k) = \frac{1}{2} \log \left(\frac{k^+}{k^-} \right)$. The rapidity gaps $\Delta y_{1,2}$ can be calculated as:

$$\Delta y_{1,2} = \log \left[\frac{M_{T\mathcal{A}}}{|\mathbf{k}_{T1,2}|} \frac{1 - z_{1,2}}{z_{1,2} - \frac{\mathbf{k}_{T2,1}^2}{s(1-z_{2,1})}} \right].$$

From this expression, taken together with the conditions (3) and (4), one can see, that the following hierarchy holds in the MRK limit:

$$\frac{\mathbf{k}_{T1,2}^2}{s} \ll z_1 \sim z_2 \ll 1, \quad (5)$$

so that the small parameters, which control the MRK limit are actually $z_{1,2}$, while the transverse momenta are of the same order of magnitude as the hard scale, and the collinear asymptotic of the amplitude (2) is inapplicable. Also, the following scaling relations for momentum components hold in the MRK limit:

$$M_{T\mathcal{A}} \sim |\mathbf{k}_{T1}| \sim q_1^+ \sim O(z_1) \gg q_1^- \sim O(z_1^2), \quad M_{T\mathcal{A}} \sim |\mathbf{k}_{T2}| \sim q_2^- \sim O(z_2) \gg q_2^+ \sim O(z_2^2), \quad (6)$$

which allows one to neglect the “small” light-cone components of momenta q_1^- and q_2^+ .

The systematic formalism for the calculation of the asymptotic expressions for arbitrary QCD amplitudes in the MRK limit has been formulated by L. N. Lipatov and M. I. Viazovsky in a form of gauge-invariant Effective Field Theory (EFT) for Multi-Regge processes in QCD [9, 10], see also [11] for a review. The MRK asymptotics of the amplitude in this EFT is constructed from gauge-invariant blocks – *effective vertices*, which describe the production of clusters of QCD partons, separated by the large rapidity gaps. These effective vertices are connected together via t -channel exchanges of gauge-invariant off-shell degrees of freedom, Reggeized gluons R_\pm and Reggeized quarks Q_\pm . The latter obey special kinematical constraints, such that the field $Q_\pm(R_\pm)$ carries only q^\pm light-cone component of momentum and the transverse momentum of the same order of magnitude, while $q^\mp = 0$. As it was shown above, these kinematical constraints are equivalent to MRK.

Due to the requirements of gauge-invariance of effective vertices and the above-mentioned kinematic constraints, the interactions of QCD partons and Reggeons in the EFT [9, 10] are nonlocal and contain the Wilson’s exponents of gluonic fields. After the perturbative expansion, the latter generate an infinite series of induced vertices of interaction of particles and Reggeons. The Feynman Rules of the EFT are worked out in details in the Ref. [12],

$\frac{+}{a} \dashrightarrow \frac{-}{b} = \frac{-i\delta_{ab}}{2q^2}$	$\frac{a}{q} \dashrightarrow \frac{b}{\mu} = (-iq^2)n_\mu^\mp \delta_{ab}$
	$g_s f_{aa_1 a_2} (n_\mu^\mp n_\nu^\mp) \frac{q^2}{k_1^\mp}$
	$ig_s^2 (n_{\mu_1}^\mp n_{\mu_2}^\mp n_{\mu_3}^\mp) \frac{q^2}{k_3^\mp} \left[\frac{f_{aba_1} f_{ba_2 a_3}}{k_1^\mp} + \frac{f_{aba_2} f_{ba_1 a_3}}{k_2^\mp} \right]$

FIG. 1: Feynman rules of the EFT [9]. Propagator of the Reggeized gluon (top-left panel) and Reggeon-gluon induced vertices up to the $O(g_s^2)$ are shown. The usual Feynman Rules of QCD hold for interactions of ordinary quarks and gluons.

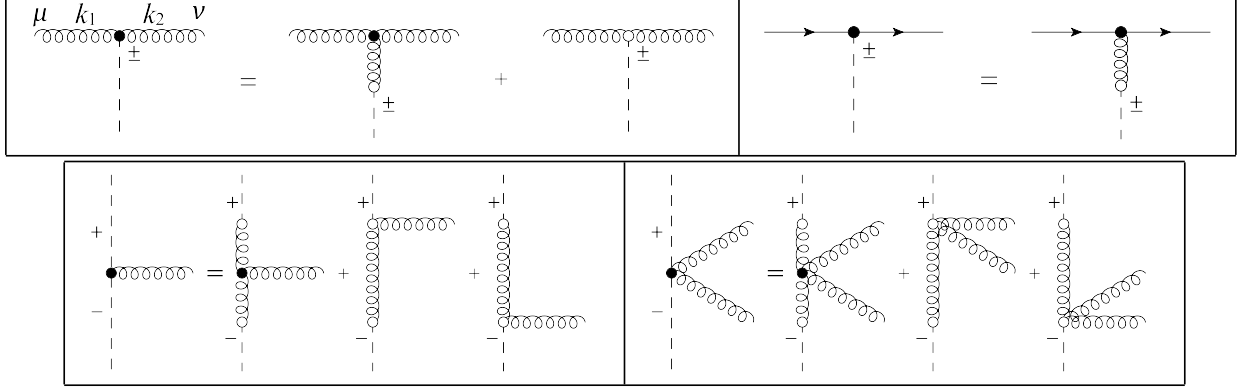


FIG. 2: Structure of the effective vertices $R_\pm gg$ (top-left), $R_\pm q\bar{q}$ (top-right), $R_+ R_- g$ (bottom-left) and the $R_+ R_- gg$ combined vertex (bottom-right). These vertices appear in the diagrams of the Figs. 3, 5 and 6.

however we also collect the induced and effective vertices, relevant for our present study in the Figs. 1 and 2 for the reader's convenience.

The diagrammatic representation of the squared amplitude of the process (1) is shown in the Fig. 3. Explicitly, the $R_\pm gg$ effective vertex, which is depicted diagrammatically in the Fig. 2, reads:

$$\Gamma_{\mu\nu\pm}^{abc}(k_1, k_2) = -ig_s f^{abc} \left[2g_{\mu\nu} k_1^\mp + (2k_2 + k_1)_\mu n_\nu^\mp - (2k_1 + k_2)_\nu n_\mu^\mp - \frac{(k_1 + k_2)^2}{k_1^\mp} n_\mu^\mp n_\nu^\mp \right].$$

Evaluating the square of $R_\pm gg$ effective vertex, contracted with the polarization vectors of

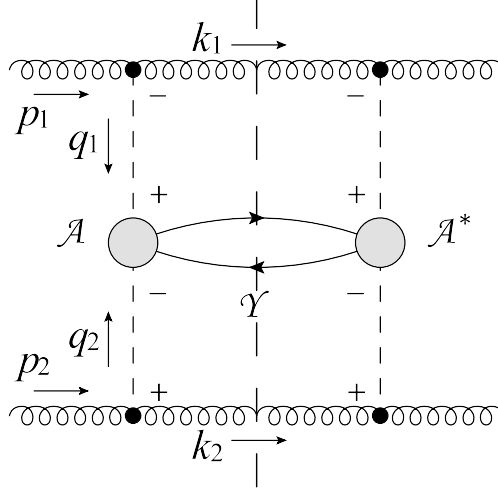


FIG. 3: Diagrammatic representation of the MRK asymptotics for squared amplitude of the subprocess (1).

on-shell external gluons one obtains:

$$\sum_{\lambda_1, \lambda_2} |\Gamma_{\mu\nu\pm}(k_1, -k_2) \epsilon_\mu(k_1, \lambda_1) \epsilon_\nu^*(k_2, \lambda_2)|^2 = 8(k_1^\mp)^2. \quad (7)$$

Using the result (7) and the Feynman rules of the Fig. 1 one can write the MRK asymptotics of the squared amplitude of the process (1) in the following form:

$$|\overline{\mathcal{M}}|^2_{\text{MRK}} \simeq \frac{4g_s^4}{\mathbf{k}_{T1}^2 \mathbf{k}_{T2}^2} \tilde{P}_{gg}(z_1) \tilde{P}_{gg}(z_2) \frac{|\overline{\mathcal{A}_{PRA}}|^2}{z_1 z_2}, \quad (8)$$

where the MRK gluon-gluon splitting functions $\tilde{P}_{gg}(z) = 2C_A/z$ reproduce the small- z asymptotics of the full DGLAP splitting functions and the squared PRA amplitude is defined as:

$$|\overline{\mathcal{A}_{PRA}}|^2 = \left(\frac{q_1^+ q_2^-}{4(N_c^2 - 1)\sqrt{t_1 t_2}} \right)^2 [\mathcal{A}_{c_1 c_2}^* \mathcal{A}^{c_1 c_2}], \quad (9)$$

where \mathcal{A} is the Green's function of the subprocess $R_+(q_1) + R_-(q_2) \rightarrow \mathcal{Y}(P_A)$ with amputated propagators of the Reggeized gluons, and $c_{1,2}$ are their color indices. The error of the approximation (8) is suppressed as $O(z_{1,2})$ w. r. t. the leading term.

In contrast with the collinear limit, PRA amplitude explicitly and nontrivially depends on the \mathbf{q}_{T1} and \mathbf{q}_{T2} . However, when $\mathbf{k}_{T1,2} \ll \mu^2$, MRK limit reduces to the small- $z_{1,2}$ asymptotics of the collinear limit and the Eq. (8) should reproduce the Eq. (2). To this end,

the following *collinear limit constraint* for the PRA amplitude should hold:

$$\int \frac{d\phi_1 d\phi_2}{(2\pi)^2} \lim_{t_{1,2} \rightarrow 0} |\overline{\mathcal{A}_{PRA}}|^2 = |\overline{\mathcal{A}_{CPM}}|^2, \quad (10)$$

where $\phi_{1,2}$ are the azimuthal angles of the vectors $\mathbf{q}_{T1,2}$. One can prove the constraint (10) for the general PRA amplitudes of the type $R_+ + R_- \rightarrow \mathcal{Y}$, with the help of Ward identities for the Green's functions with Reggeized gluons, which has been discovered in the Ref. [13].

Now we introduce the *modified MRK (mMRK) approximation* for the squared amplitude of the subprocess (1) as follows:

1. In the Eq. (8) we substitute the MRK asymptotics for the splitting functions $\tilde{P}_{gg}(z)$ by the full LO DGLAP expression $P_{gg}(z)$.
2. We substitute the factors $\mathbf{k}_{T1,2}^2$ in the denominator of (8) by the exact value of $q_{1,2}^2$, as if all four components of momentum $q_{1,2}^+$, $q_{1,2}^-$ and \mathbf{q}_T were flowing through the t -channel propagator: $\mathbf{k}_{T1,2}^2 \rightarrow -q_{1,2}^2 = \mathbf{q}_{T1,2}^2/(1 - z_{1,2})$.
3. However, the “small” light-cone components of momenta: q_1^- and q_2^+ do not propagate into the hard scattering process, so its gauge-invariant definition is unaffected and is given by the Lipatov's EFT [9].

After these substitutions, the mMRK approximation for the squared amplitude of the subprocess (1) takes the following form:

$$|\overline{\mathcal{M}}|^2_{\text{mMRK}} \simeq \frac{4g_s^4}{q_1^2 q_2^2} P_{gg}(z_1) P_{gg}(z_2) \frac{|\overline{\mathcal{A}_{PRA}}|^2}{z_1 z_2}. \quad (11)$$

The mMRK approximation (11) reproduces the exact QCD results both in the collinear and MRK limits. The latter suggests, that it should be more accurate than the default collinear limit approximation (2) when $\mathbf{k}_{T1,2} \sim \mu^2$ even outside of the strict MRK limit $z_{1,2} \ll 1$, however at present we can not give the precise parametric estimate of accuracy of the Eq. (11) in this kinematic region. The available numerical evidence (see the Ref. [14] for the case of amplitudes with reggeized gluons in the t -channel and Refs. [15, 16] for the case of Reggeized quarks) supports the form of mMRK approximation, proposed above.

To derive the LO factorization formula of PRA we substitute the mMRK approximation (11) to the factorization formula of CPM integrated over the phase-space of additional

partons $k_{1,2}$:

$$d\sigma = \int \frac{dk_1^+ d^2 \mathbf{k}_{T1}}{(2\pi)^3 k_1^+} \int \frac{dk_2^- d^2 \mathbf{k}_{T2}}{(2\pi)^3 k_2^-} \int d\tilde{x}_1 d\tilde{x}_2 f_g(\tilde{x}_1, \mu^2) f_g(\tilde{x}_2, \mu^2) \frac{|\overline{\mathcal{M}}|_{\text{mMRK}}^2}{2S\tilde{x}_1\tilde{x}_2} \times \\ \times (2\pi)^4 \delta\left(\frac{1}{2}(q_1^+ n_- + q_2^- n_+) + q_{T1} + q_{T2} - P_A\right) d\Phi_A, \quad (12)$$

where $f_g(x, \mu^2)$ are the (integrated) Parton Distribution Functions (PDFs) of the CPM, $p_{1,2}^\mu = \tilde{x}_{1,2} P_{1,2}^\mu$, where $P_{1,2}$ are the four-momenta of colliding protons, and $d\Phi_A$ is the element of the Lorentz-invariant phase-space for the final state of the hard subprocess \mathcal{Y} .

Changing the variables in the integral: $(k_1^+, \tilde{x}_1) \rightarrow (z_1, x_1)$, $(k_2^-, \tilde{x}_2) \rightarrow (z_2, x_2)$, where $x_{1,2} = \tilde{x}_{1,2} z_{1,2}$, one can rewrite the Eq. 12 in a k_T -factorized form:

$$d\sigma = \int_0^1 \frac{dx_1}{x_1} \int \frac{d^2 \mathbf{q}_{T1}}{\pi} \tilde{\Phi}_g(x_1, t_1, \mu^2) \int_0^1 \frac{dx_2}{x_2} \int \frac{d^2 \mathbf{q}_{T2}}{\pi} \tilde{\Phi}_g(x_2, t_2, \mu^2) \cdot d\hat{\sigma}_{\text{PRA}}, \quad (13)$$

where the partonic cross-section in PRA is given by:

$$d\hat{\sigma}_{\text{PRA}} = \frac{|\overline{\mathcal{A}_{\text{PRA}}}|^2}{2Sx_1x_2} \cdot (2\pi)^4 \delta\left(\frac{1}{2}(q_1^+ n_- + q_2^- n_+) + q_{T1} + q_{T2} - P_A\right) d\Phi_A, \quad (14)$$

and the tree-level “unintegrated PDFs” (unPDFs) are:

$$\tilde{\Phi}_g(x, t, \mu^2) = \frac{1}{t} \frac{\alpha_s}{2\pi} \int_x^1 dz P_{gg}(z) \cdot \frac{x}{z} f_g\left(\frac{x}{z}, \mu^2\right). \quad (15)$$

The cross-section (13) with “unPDFs” (15) contains the collinear divergence at $t_{1,2} \rightarrow 0$ and infrared (IR) divergence at $z_{1,2} \rightarrow 1$. To regularize the latter, we observe, that the mMRK expression (11) can be expected to give a reasonable approximation for the exact matrix element only in the rapidity-ordered part of the phase-space, where $\Delta y_1 > 0$ and $\Delta y_2 > 0$. The cutoff on $z_{1,2}$ follows from this conditions:

$$z_{1,2} < 1 - \Delta_{\text{KMR}}(t_{1,2}, \mu^2), \quad (16)$$

where $\Delta_{\text{KMR}}(t, \mu^2) = \sqrt{t}/(\sqrt{\mu^2} + \sqrt{t})$, and we have taken into account that $\mu^2 \sim M_{T\mathcal{A}}^2$. The collinear singularity is regularized by the Sudakov formfactor:

$$T_i(t, \mu^2) = \exp \left[- \int_t^{\mu^2} \frac{dt'}{t'} \frac{\alpha_s(t')}{2\pi} \sum_{j=q,\bar{q},g} \int_0^1 dz z \cdot P_{ji}(z) \theta(1 - \Delta_{\text{KMR}}(t', \mu^2) - z) \right], \quad (17)$$

which resums doubly-logarithmic corrections $\sim \log^2(t/\mu^2)$ in the LLA in a way similar to what is done in the standard PS [17].

The final form of our unPDF is:

$$\Phi_i(x, t, \mu^2) = \frac{T_i(t, \mu^2)}{t} \frac{\alpha_s(t)}{2\pi} \sum_{j=q, \bar{q}, g} \int_x^1 dz P_{ij}(z) \cdot \frac{x}{z} f_j\left(\frac{x}{z}, t\right) \cdot \theta\left(1 - \Delta_{KMR}(t, \mu^2) - z\right), \quad (18)$$

which coincides with Kimber, Martin and Ryskin (KMR) unPDF [18]. The KMR unPDF is actively used in the phenomenological studies employing k_T -factorization, but to our knowledge, the reasoning above is the first systematic attempt to uncover its relationships with MRK limit of the QCD amplitudes.

The KMR unPDF approximately (see Sec. 2 of the Ref. [19] for the further details) satisfies the following normalization condition:

$$\int_0^{\mu^2} dt \Phi_i(x, t, \mu^2) = x f_i(x, \mu^2), \quad (19)$$

which ensures the normalization for the single-scale observables, such as proton structure functions or $d\sigma/dQ^2 dy$ cross-section in the Drell-Yan process, on the corresponding LO CPM results up to power-suppressed corrections and terms of the NLO in α_s . Results for multiscale observables in PRA are significantly different than in CPM, due to the nonzero transverse-momenta of partons in the initial state.

The main difference of PRA from the multitude of studies in the k_T -factorization, such as Ref. [8], is the application of matrix elements with off-shell initial-state partons (Reggeized quarks and gluons) from Lipatov's EFT [9, 10], which allows one to study the arbitrary processes involving non-Abelian structure of QCD without violation of gauge-invariance due to the nonzero virtuality of initial-state partons. This approach, together with KMR unPDF gives stable and consistent results in a wide range of phenomenological applications, which include the description of the angular correlations of dijets [20], b -jets [21], charmed [22, 23] and bottom-flavoured [24] mesons, different multiscale observables in hadroproduction of diphotons [16] and photoproduction of photon+jet pairs [25], as well as some other examples.

Recently, the new approach to derive gauge-invariant scattering amplitudes with off-shell initial-state partons, using the spinor-helicity techniques and BCFW-like recursion relations for such amplitudes has been introduced in the Refs. [26, 27]. This formalism is equivalent to the Lipatov's EFT at the tree level, but for some observables, e. g. related with heavy quarkonia, or for the generalization of the formalism to NLO, the explicit Feynman rules and the structure of EFT is more convenient.

III. LO PRA MERGED WITH TREE-LEVEL NLO CORRECTIONS

Let's consider the kinematic conditions of a measurement in the Ref. [3]. In this experiment, the events with at least one jet having $p_T^{\text{jet}} > p_{TL}^{\text{min}}$ has been recorded in pp -collisions at the $\sqrt{S} = 7$ TeV, and the semileptonic decays of B -hadrons where reconstructed in this events, through the decay vertices, displaced w. r. t. the primary pp -collision vertex. The B -hadron is required to have $p_{TB} > p_{TB}^{\text{min}} = 15$ GeV, while three data-samples are presented in the Ref. [3] for three values of $p_{TL}^{\text{min}} = 56, 84$ and 120 GeV. The rapidities of B -hadrons are constrained to be $|y_B| < y_B^{\text{max}} = 2$, while the leading jet is searched in somewhat wider domain $|y_{\text{jet}}| < y_{\text{jet}}^{\text{max}} = 3$.

The leading jet, reconstructed in this experiment, sets the hard scale of the event. Two possibilities should be considered: the first one is, that the jet originating from b -quark or \bar{b} -antiquark is the leading one, and the second option is, that some gluon or light-quark jet is leading in p_T , and jets originating from b or \bar{b} are subleading. Observables with such kinematic constraints on the QCD radiation are difficult to study in k_T -factorization, because the radiation of additional hard partons is already taken into account in the unPDFs, and the jet, originating from unPDF could happen to be the leading one.

One can easily estimate the distribution of additional jets in rapidity, using the KMR model for unPDFs (18). The variable z is related with rapidity (y) of the parton, emitted on the last step of the parton cascade, as follows:

$$z(y) = \left(1 + \frac{\sqrt{t}}{x\sqrt{S}}e^y\right)^{-1},$$

so, starting from Eq. (18) one can derive the distribution integrated over t from some scale t_0 up to μ^2 , but unintegrated over y : $G_i(x, y, t_0, \mu^2)$. Representative plots of this distribution for the case of P_{gg} -splitting only, are shown in the Fig. 4 for some values of scales typical for the process under consideration. The LO PDFs from the MSTW-2008 set [28] has been used to produce this plot.

From Fig. 4 it is clear, that in the KMR model, the majority of hardest ISR jets jets with $\mathbf{k}_T^2 \sim \mu^2$ lie within the rapidity interval $|y| < 3$ if the particles, produced in the primary hard process have rapidities close to zero. Therefore this jets can be identified as the leading ones. But the kinematic approximations, which has been made in the derivation of the factorization formula, are least reliable in this region of phase-space, and hence the poor

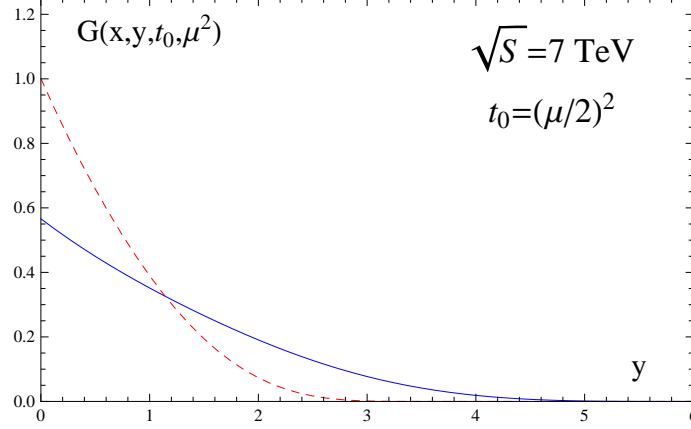


FIG. 4: Distribution in rapidity of a gluon jets with $|\mathbf{k}_T| > \mu/2$ from the last stage of the parton cascade, as given by the KMR model (18). Solid line – $\mu^2 = 10^3 \text{ GeV}^2$, dashed line – $\mu^2 = 10^5 \text{ GeV}^2$. Both plots are normalized to the common integral, scale of the G -axis is arbitrary. For both distributions: $x = \mu/\sqrt{S}$, i. e. the rapidity of the hard process is zero.

agreement with data is to be expected. To avoid the above-mentioned problem, we will merge the LO PRA description of events with the leading $b(\bar{b})$ -jets with events triggered by the leading gluon jet, originating from the exact $2 \rightarrow 3$ NLO PRA matrix element.

The LO ($O(\alpha_s^2)$) subprocess, which we will take into account is:

$$R_+(q_1) + R_-(q_2) \rightarrow b(q_3)(\rightarrow B(p_{TB})) + \bar{b}(q_4)(\rightarrow \bar{B}(p_{T\bar{B}})), \quad (20)$$

where the hadronization of $b(\bar{b})$ -quarks into the $B(\bar{B})$ mesons is described by the set of universal, scale-dependent parton-to-hadron fragmentation functions, fitted on the world data on the B -hadron production in e^+e^- -annihilation in the Ref. [29].

The following kinematic cuts are applied to the LO subprocess (20):

1. Both B and \bar{B} mesons are required to have $|y_B| < y_B^{\max}$ and $\min(p_{TB}, p_{T\bar{B}}) > p_{TB}^{\min}$.
2. If the distance between three-momenta \mathbf{q}_3 and \mathbf{q}_4 in the $(\Delta y, \Delta\phi)$ -plane: $\Delta R_{34} = \sqrt{\Delta y_{34}^2 + \Delta\phi_{34}^2} > \Delta R_{\text{exp.}} = 0.5$, then b and \bar{b} jets are resolved separately and we define: $p_{TL} = \max(|\mathbf{q}_{T3}|, |\mathbf{q}_{T4}|)$.
3. If $\Delta R_{34} < \Delta R_{\text{exp.}}$, then $p_{TL} = |\mathbf{q}_{T3} + \mathbf{q}_{T4}|$, according to the anti- k_T jet clustering algorithm [30].

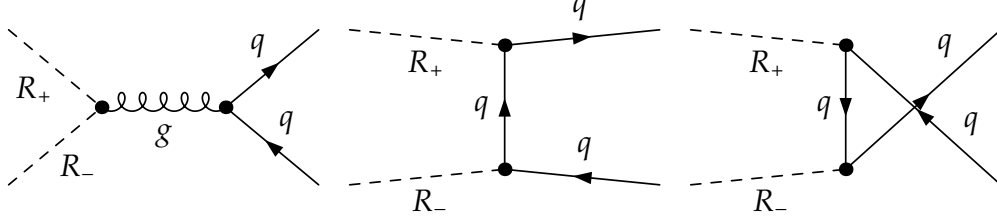


FIG. 5: The Feynman diagrams of Lipatov's EFT for the Reggeized amplitude of subprocess $R_+ + R_- \rightarrow b + \bar{b}$.

4. The MC event is *accepted* if $\max(|\mathbf{q}_{T1}|, |\mathbf{q}_{T2}|) < p_{TL}$ and $p_{TL} > p_{TL}^{\min}$.

The set of Feynman diagrams for the subprocess (20) is presented in the Fig. 5. The convenient expression for the squared amplitude of this subprocess with massless quarks can be found in the Ref. [20]. Due to the Ward identities of the Ref. [13], this amplitude coincides with the amplitude, which can be obtained in the “old k_T -factorization” prescription, i. e. by substituting the polarization vectors of initial-state gluons in the usual $gg \rightarrow q\bar{q}$ amplitude by $q_{T1,2}^\mu/|\mathbf{q}_{T1,2}|$.

The NLO ($O(\alpha_s^3)$) subprocess is

$$R_+(q_1) + R_-(q_2) \rightarrow b(q_3)(\rightarrow B(p_{TB})) + \bar{b}(q_4)(\rightarrow \bar{B}(p_{T\bar{B}})) + g(q_5), \quad (21)$$

and the following kinematic constraints are applied in the calculation of this contribution:

1. Both B and \bar{B} mesons are required to have $|y_B| < y_B^{\max}$ and $\min(p_{TB}, p_{T\bar{B}}) > p_{TB}^{\min}$.
2. Gluon jet is the leading one: $p_{TL} = |\mathbf{q}_{T5}|$, $\max(|\mathbf{q}_{T1}|, |\mathbf{q}_{T2}|, |\mathbf{q}_{T3}|, |\mathbf{q}_{T4}|) < p_{TL}$ and $p_{TL} > p_{TL}^{\min}$.
3. Rapidity of the gluon is required to be $|y_5| < y_{\text{jet}}^{\max}$. The gluon jet is isolated: $\Delta R_{35} > \Delta R_{\text{exp.}}$ and $\Delta R_{45} > \Delta R_{\text{exp.}}$.

Furthermore, since the matrix elements for both subprocesses (20) and (21) are taken in the approximation of massless b -quarks, the corresponding final-state collinear singularity is regularized by the condition $(q_3 + q_4)^2 > 4m_b^2$, where $m_b = 4.5$ GeV.

Few comments are in order. For the both subprocesses (20) and (21), transverse momenta of jets from the unPDFs are constrained to be subleading. In such a way we avoid the double-counting of the leading emissions between LO and NLO contributions and additional

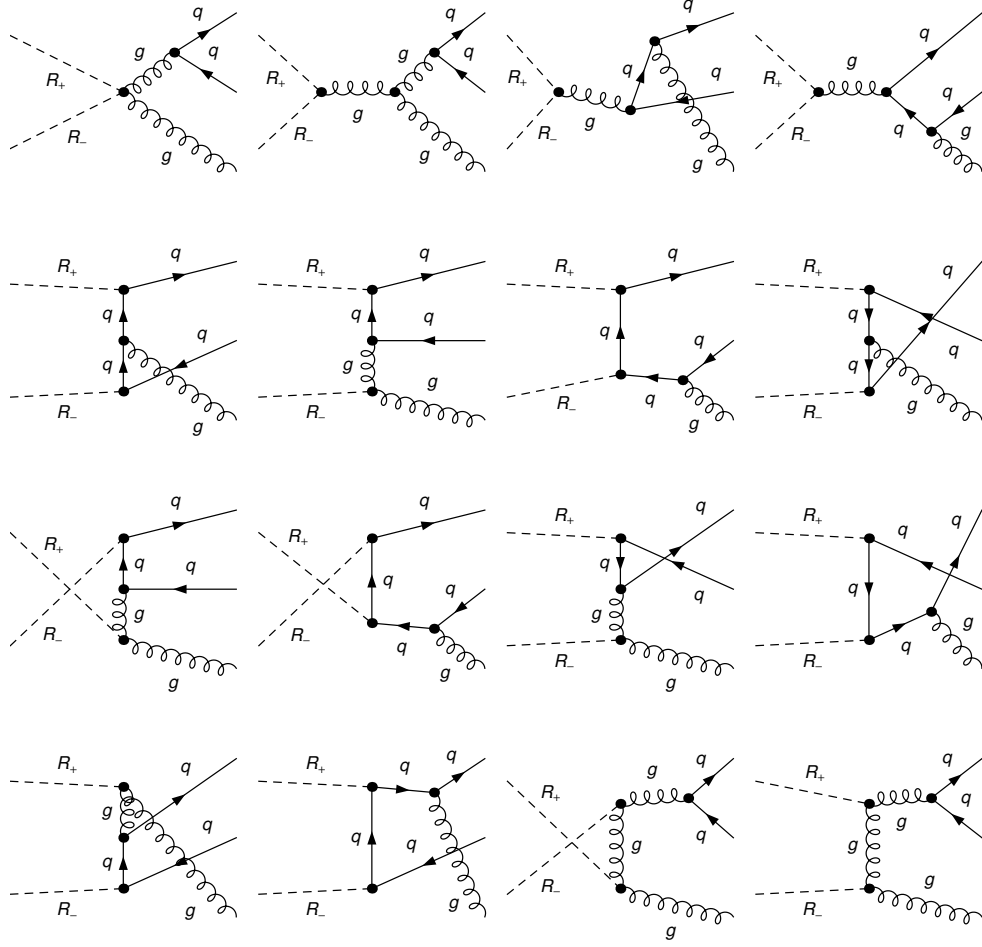


FIG. 6: The Feynman diagrams of Lipatov's EFT for the Reggeized amplitude of subprocess $R_+ + R_- \rightarrow b + \bar{b} + g$.

subtractions are not needed. This is in contrast to the observables fully inclusive in the QCD radiation [16], where the double-counting subtractions between LO and NLO terms has to be done. Another comment concerns the isolation condition for the leading gluon jet in the NLO contribution (21). This condition regularizes the collinear singularity between the final-state gluon and $b(\bar{b})$ -quark. In the full NLO calculation, this singularity will be cancelled by the loop correction, producing some finite contribution, but since the gluon is required to be harder than b or \bar{b} -quarks, this finite contribution will be proportional to the $P_{gq}(z) = C_F(1 + (1 - z)^2)/z$ splitting function at $z \rightarrow 1$, so we don't expect the logarithmically-enhanced contributions from this region of the phase-space.

The set of Feynman diagrams for amplitude of the subprocess (21) is presented in the

Fig. 6. We generate this amplitude, using our model-file **ReggeQCD**, which implements the Feynman rules of Lipatov's EFT in **FeynArts** [31]. The squared amplitude is computed using the **FormCalc** [32] package, and has been compared numerically with the squared amplitude, obtained by the methods of the Refs. [26, 27]. Our results and results of Ref. [26, 27] agree up to machine precision. Apart from the Feynman rules, depicted in the Figs. 1 and 2, **ReggeQCD** package contains all Feynman rules, which are needed to generate arbitrary PRA amplitude with reggeized gluons or quarks in the initial state and up to three quarks, gluons or photons in the final state. We are planning to publish the **ReggeQCD** model-file in a separate paper [33]. The **FORTTRAN** code for the squared amplitudes of the processes (20) and (21) is available from authors by request.

As it was stated above, we will use the fragmentation model, to describe hadronization of b -quarks into B -hadrons, so the observable cross-section is:

$$\begin{aligned} \frac{d\sigma_{\text{obs.}}}{dy_B dy_{\bar{B}} d\Delta\phi} &= \int_{p_{TB}^{\min}}^{\infty} dp_{TB} \int_{p_{T\bar{B}}^{\min}}^{\infty} dp_{T\bar{B}} \int_0^1 \frac{dz_1}{z_1} D_{B/b}(z_1, \mu^2) \int_0^1 \frac{dz_2}{z_2} D_{B/b}(z_2, \mu^2) \\ &\times \frac{d\sigma_{b\bar{b}}}{dq_{T3} dq_{T4} dy_3 dy_4 d\Delta\phi}, \end{aligned} \quad (22)$$

where $\Delta\phi = \Delta\phi_{34}$, $D_{B/b}(z, \mu^2)$ are the fragmentation functions [29], and $q_{T3} = |\mathbf{q}_{T3}| = p_{TB}/z_1$, $q_{T4} = |\mathbf{q}_{T4}| = p_{T\bar{B}}/z_2$, $y_3 = y_B$, $y_4 = y_{\bar{B}}$. To simplify the numerical calculations, it is very convenient to integrate over $q_{T3,4}$ instead of p_{TB} and $p_{T\bar{B}}$ in Eq. (22), then all the dependence of the cross-section on fragmentation functions can be absorbed into the following measurement function:

$$\Theta(\tilde{z}, \mu^2) = \begin{cases} \int_{1/\tilde{z}}^1 dz D_{B/q}(z, \mu^2) & \text{if } \tilde{z} > 1, \\ 0 & \text{otherwise,} \end{cases} \quad (23)$$

which can be efficiently computed and tabulated in advance, therefore reducing the dimension of phase-space integrals by 2. Then the master-formula for the cross-section of $2 \rightarrow 2$ subprocess (20) in PRA takes the form:

$$\begin{aligned} \frac{d\sigma_{\text{obs.}}^{(2 \rightarrow 2)}}{dy_B dy_{\bar{B}} d\Delta\phi} &= \int_0^{\infty} dq_{T3} dq_{T4} \cdot \Theta\left(\frac{q_{T3}}{p_{TB}^{\min}}, \mu^2\right) \Theta\left(\frac{q_{T4}}{p_{T\bar{B}}^{\min}}, \mu^2\right) \\ &\times \int_0^{\infty} dt_1 \int_0^{2\pi} d\phi_1 \Phi_g(x_1, t_1, \mu^2) \Phi_g(x_2, t_2, \mu^2) \cdot \frac{q_{T3} q_{T4}}{2(2\pi)^3 (Sx_1 x_2)^2} \cdot \frac{|\overline{\mathcal{A}_{PRA}^{(2 \rightarrow 2)}}|^2}{\theta_{\text{cuts}}^{(2 \rightarrow 2)}}, \end{aligned} \quad (24)$$

where ϕ_1 is azimuthal angle between the vector \mathbf{q}_{T1} and \mathbf{q}_{T3} , $t_2 = |\mathbf{q}_{T3} + \mathbf{q}_{T4} - \mathbf{q}_{T1}|$, $x_1 = (q_3^+ + q_4^+)/\sqrt{S}$, $x_2 = (q_3^- + q_4^-)/\sqrt{S}$, and the theta-function $\theta_{\text{cuts}}^{(2 \rightarrow 2)}$ implements the kinematic constraints for $2 \rightarrow 2$ process, described above. Analogously, the formula for differential cross-section of the $2 \rightarrow 3$ process (21) reads:

$$\begin{aligned} \frac{d\sigma_{\text{obs.}}^{(2 \rightarrow 3)}}{dy_B dy_{\bar{B}} d\Delta\phi dy_5} &= \int_0^\infty dq_{T3} dq_{T4} \cdot \Theta\left(\frac{q_{T3}}{p_{TB}^{\min}}, \mu^2\right) \Theta\left(\frac{q_{T4}}{p_{TB}^{\min}}, \mu^2\right) \\ &\times \int_0^\infty dt_1 dt_2 \int_0^{2\pi} d\phi_1 d\phi_2 \Phi_g(x_1, t_1, \mu^2) \Phi_g(x_2, t_2, \mu^2) \cdot \frac{q_{T3} q_{T4} \left[\overline{\mathcal{A}_{PRA}^{(2 \rightarrow 3)}}\right]^2}{8(2\pi)^6 (S x_1 x_2)^2} \cdot \theta_{\text{cuts}}^{(2 \rightarrow 3)}, \end{aligned} \quad (25)$$

where ϕ_2 is the azimuthal angle between the vectors \mathbf{q}_{T2} , and \mathbf{q}_{T3} , $\mathbf{q}_{T5} = \mathbf{q}_{T1} + \mathbf{q}_{T2} - \mathbf{q}_{T3} - \mathbf{q}_{T4}$, $x_1 = (q_3^+ + q_4^+ + q_5^+)/\sqrt{S}$, $x_2 = (q_3^- + q_4^- + q_5^-)/\sqrt{S}$ and the theta-function $\theta_{\text{cuts}}^{(2 \rightarrow 3)}$ implements kinematic cuts for $2 \rightarrow 3$ process, described after the Eq. (21).

IV. NUMERICAL RESULTS FOR $B\bar{B}$ -CORRELATION OBSERVABLES

Now we are in a position to compare our numerical results, obtained in the approximation, formulated in the Sec. III of the present paper, to the experimental data of the Ref. [3]. Experimental uncertainties, related with the shape of $\Delta\phi$ and $\Delta R = \Delta R_{34}$ distributions are relatively small ($\sim 20 - 30\%$). They are indicated by the error-bars in the Figs. 7 and 8. However, an additional uncertainty in the absolute normalization of the cross-sections $\simeq \pm 47\%$ is reported in the Ref. [3], and it is not included into the error bars of the experimental points in the Figs. 7 and 8, as well as in the plots presented in the experimental paper. Taking this large uncertainty into account, it is reasonable to consider the overall normalization of the cross-section to be a free parameter, which is also the case in MC simulations presented in the Ref. [3]. Following this route we find, that to obtain a very good agreement of the central curve of our predictions both with the shape and normalization of all experimental spectra we have to multiply all our predictions on the universal factor $\simeq 0.4$. Since the major part of the reported normalization uncertainty is due to the uncertainty in the efficiency of identification of B -mesons, our finding seems to support the assumption, that the B -meson reconstruction efficiency is largely independent from the kinematics of the leading jet, and in particular, from the value of p_{TL}^{\min} . In the plots below, we show theoretical predictions multiplied by the above-mentioned factor, however our default result is also compatible

with experiment, if one takes into account full experimental uncertainties and the scale-uncertainty of our predictions.

In the Figs. 7 and 8 we present the comparison of our predictions with $\Delta\phi$ and ΔR spectra from the Ref. [3]. Apart from the above-mentioned overall normalization uncertainty, our model does not contain any free parameters. To generate the gluon unPDF, according to the Eq. (18) we use the LO PDFs from the MSTW-2008 set [28]. We also use the value of $\alpha_s(M_Z) = 0.1394$ from the PDF fit. In both LO (20) and NLO (21) contributions we set the renormalization and factorization scales to be equal to the p_T of the leading jet: $\mu_R = \mu_F = \xi p_{TL}$, where $\xi = 1$ for the central lines of our predictions, and we vary $1/2 < \xi < 2$ to estimate the scale-uncertainty of our prediction, which is shown in the following figures by the gray band. All numerical calculations has been performed using the adaptive MC integration routines from the CUBA library [34], mostly using the SUAVE algorithm, but with the cross-checks against the results obtained by VEGAS and DIVONNE routines.

The shape of measured distributions, both in $\Delta\phi$ and ΔR , agrees with our theoretical predictions within the experimental uncertainty. Also, our model correctly describes the dependence of the cross-section on the p_{TL}^{\min} cut.

Our predictions for the $d\sigma/d\Delta\phi$ and $d\sigma/d\Delta R$ spectra at $\sqrt{S} = 13$ TeV are presented in the Figs. 9 and 10 for the same kinematic cuts as in the Ref. [3]. Also in the Figs. 11 and 12 we provide predictions for the ratios of $\Delta\phi$ and ΔR spectra at different energies, as it was proposed in the Ref. [35]. The primary advantage of such observable is, that the theoretical scale-uncertainty mostly cancels in the ratio, leading to the more precise prediction. The residual $\Delta\phi$ and ΔR dependence of the ratio arises in the inerplay between the x -dependence of PDFs and the dynamics of emissions of additional hard radiation, therefore probing the physics of interest for PRA. Measurements of such observables at the LHC will present an important challenge for the state-of-the-art calculations in perturbative QCD and tuning of the MC event generators.

V. CONCLUSIONS

In the present paper, the example of $B\bar{B}$ -azimuthal decorrelations is used to show, how the contributions of $2 \rightarrow 2$ and $2 \rightarrow 3$ processes in PRA can be consistently taken together

to describe multiscale correlational observables in a presence of experimental constraints on additional QCD radiation. Our numerical results agree well with experimental data of the Ref. [3], up to a common normalization factor. The predictions for $\sqrt{S} = 13$ TeV are provided. Also the foundations of the Parton Reggeization Approach has been reviewed in the Sec. II and the relation of PRA with collinear and Multi-Regge limits of scattering amplitudes in QCD is highlighted.

VI. ACKNOWLEDGEMENTS

We are grateful to A. van Hameren for help in comparison of squared amplitudes obtained in the PRA with ones obtained using recursion techniques of the Refs. [26, 27]. The work was supported by the Ministry of Education and Science of Russia under Competitiveness Enhancement Program of Samara University for 2013-2020, project 3.5093.2017/8.9. The Feynman diagrams in the Figs. 1, 2 and 3 were made using JAXODRAW [36].

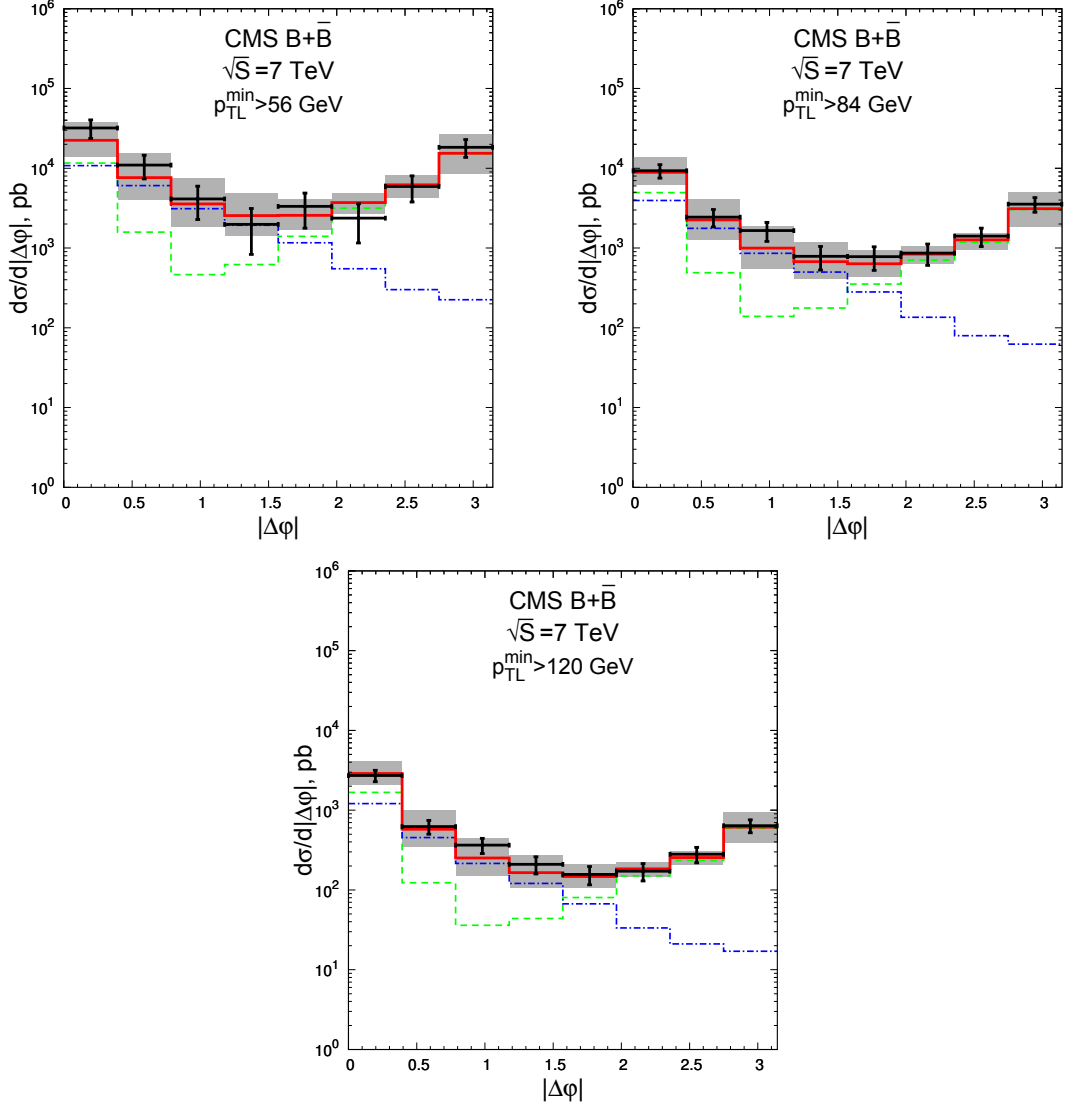


FIG. 7: Comparison of the predictions for $\Delta\phi$ -spectra of $B\bar{B}$ -pairs with the CMS data [3]. Dashed line – contribution of the LO subprocess (20), dash-dotted line – contribution of the NLO subprocess (21), solid line – sum of LO and NLO contributions.

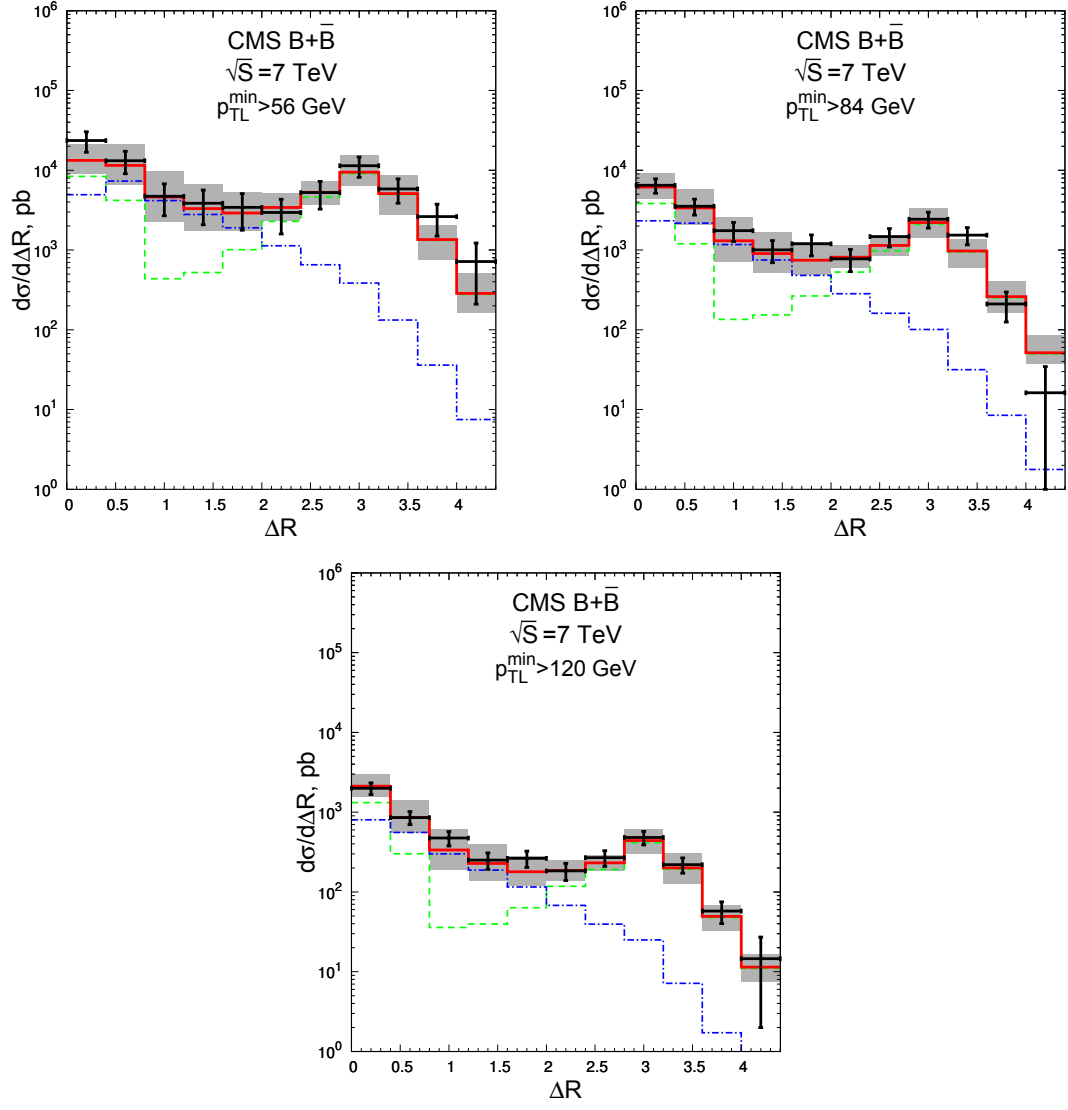


FIG. 8: Comparison of the predictions for ΔR -spectra of $B\bar{B}$ -pairs with the CMS data [3]. Notation for the histograms is the same as in the Fig. 7.

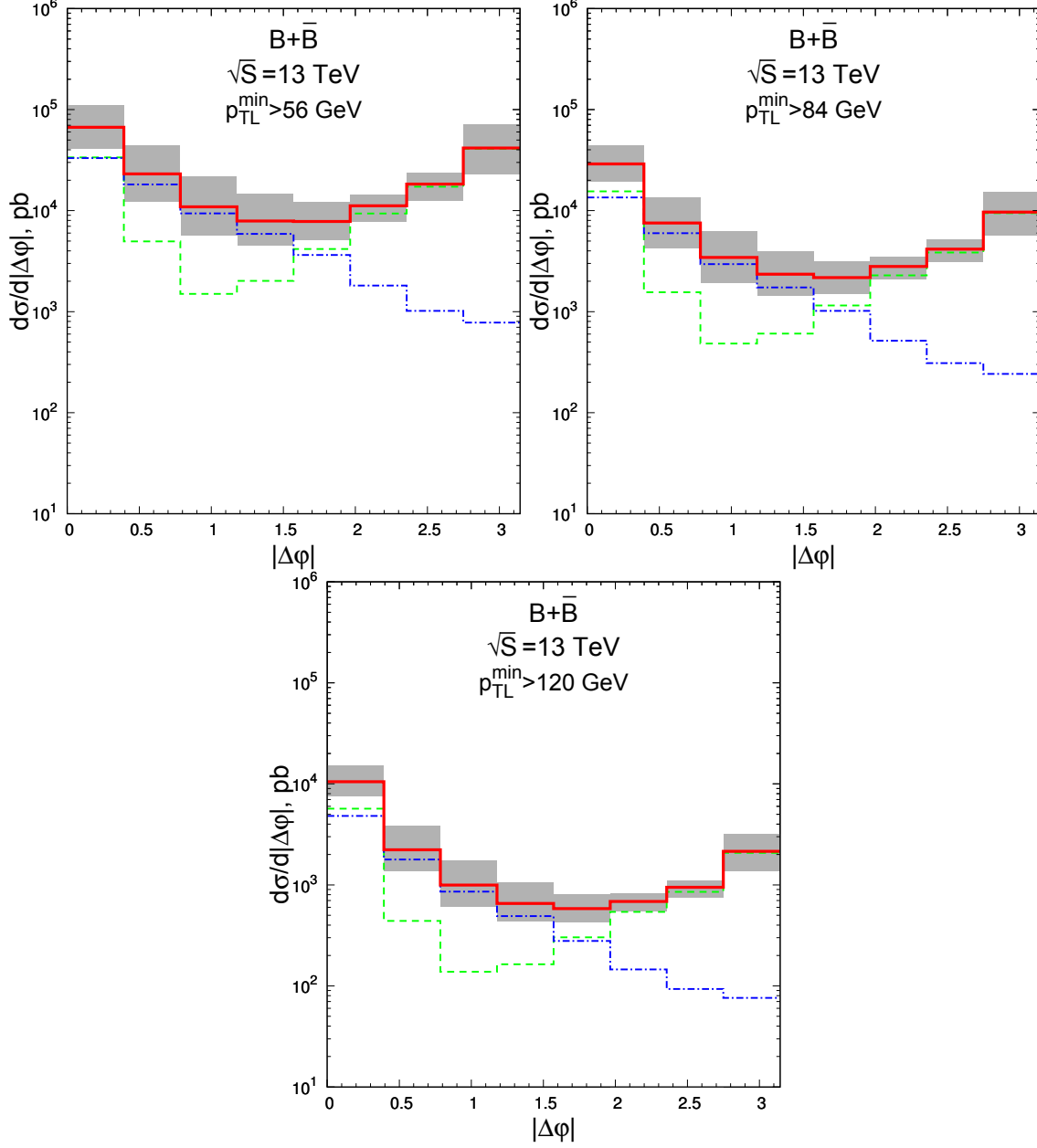


FIG. 9: Predictions for the $d\sigma/d\Delta\phi$ -spectra $\sqrt{S} = 13$ TeV for the same kinematic cuts as in the Ref. [3]. Notation for the histograms is the same as in the Fig. 7.

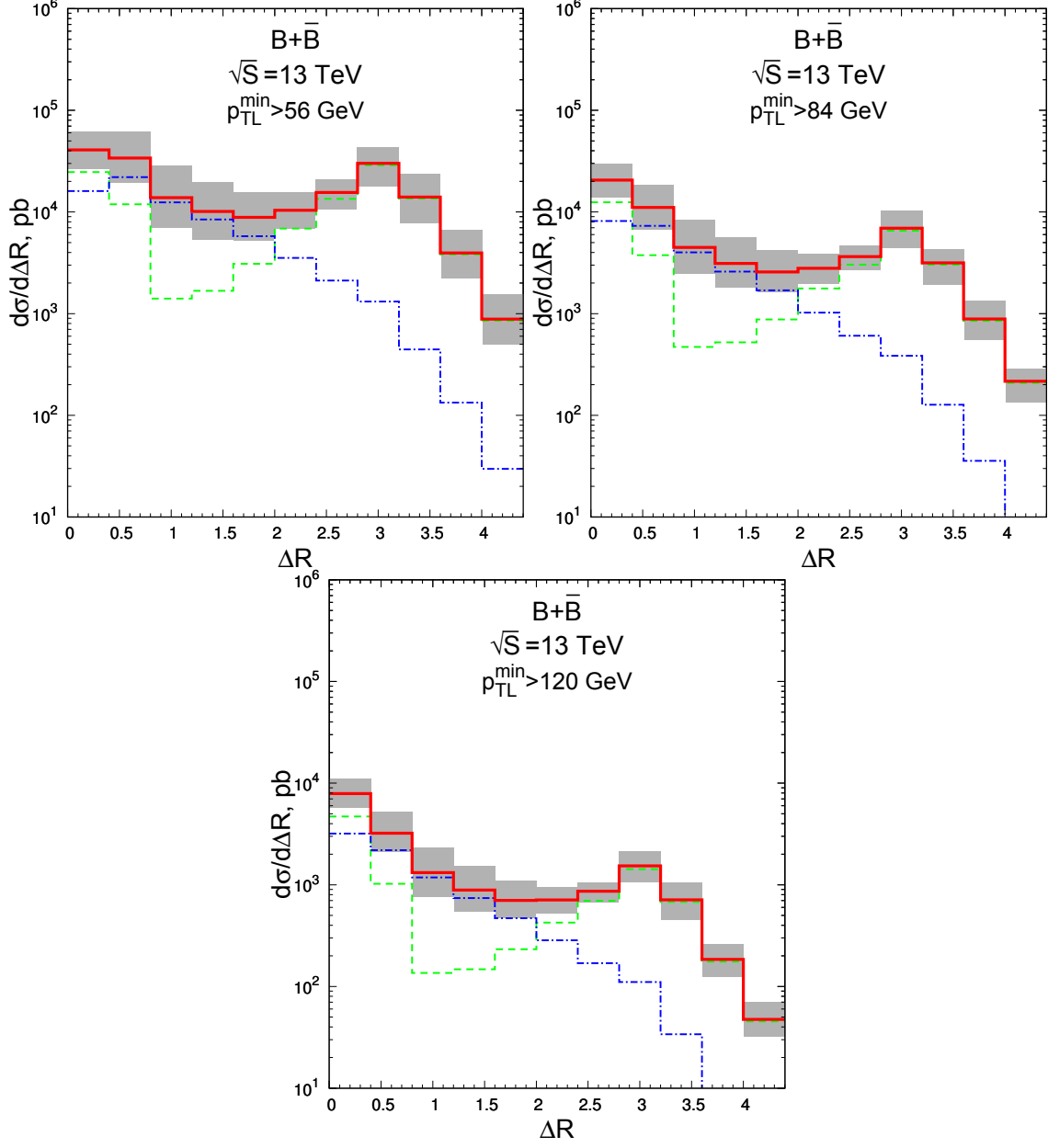


FIG. 10: Predictions for the $d\sigma/d\Delta R$ -spectra $\sqrt{S} = 13$ TeV for the same kinematic cuts as in the Ref. [3]. Notation for the histograms is the same as in the Fig. 7.

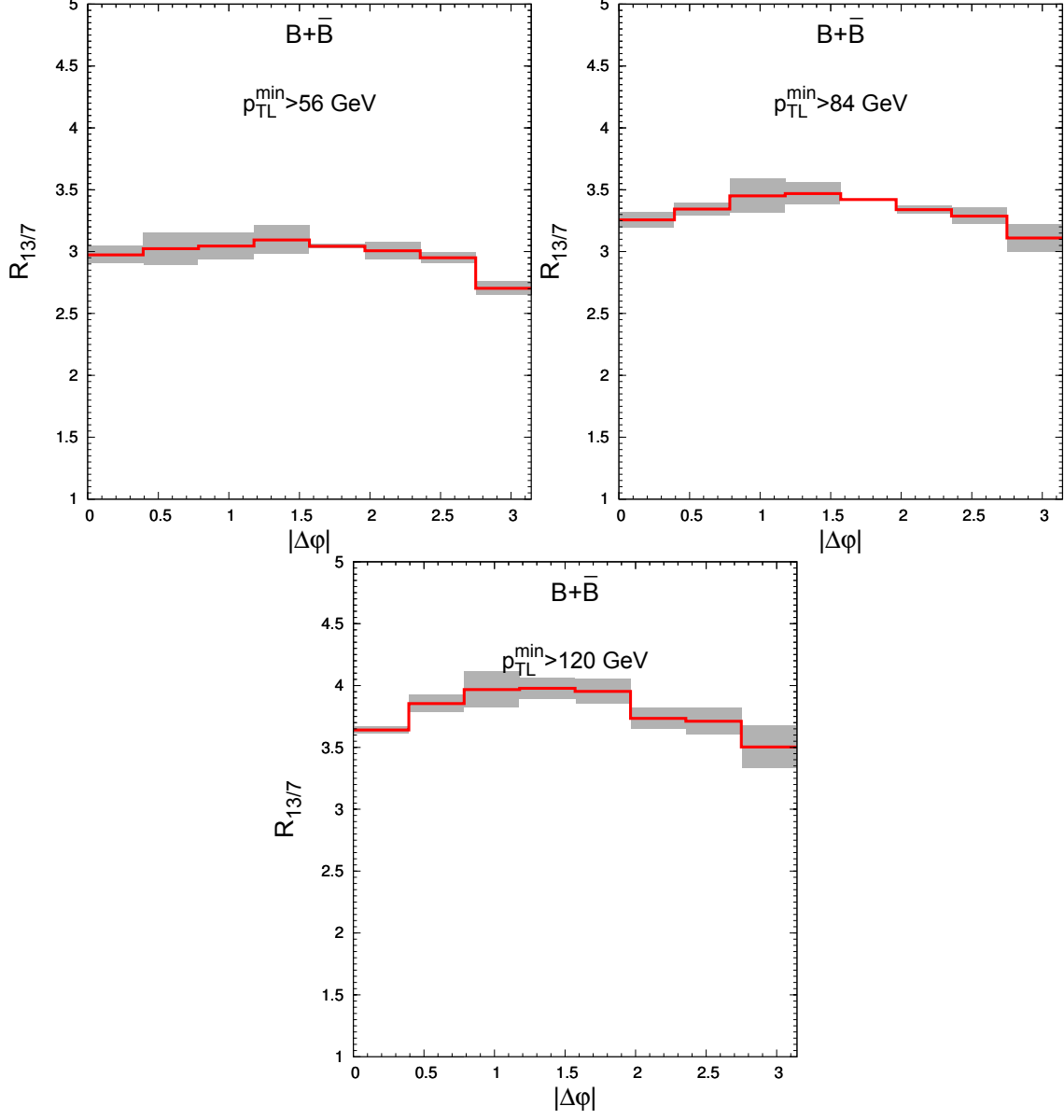


FIG. 11: Predictions for the ratio of $d\sigma/d\Delta\phi$ -spectra at $\sqrt{S} = 13$ TeV and $\sqrt{S} = 7$ TeV for the same kinematic cuts as in the Ref. [3].

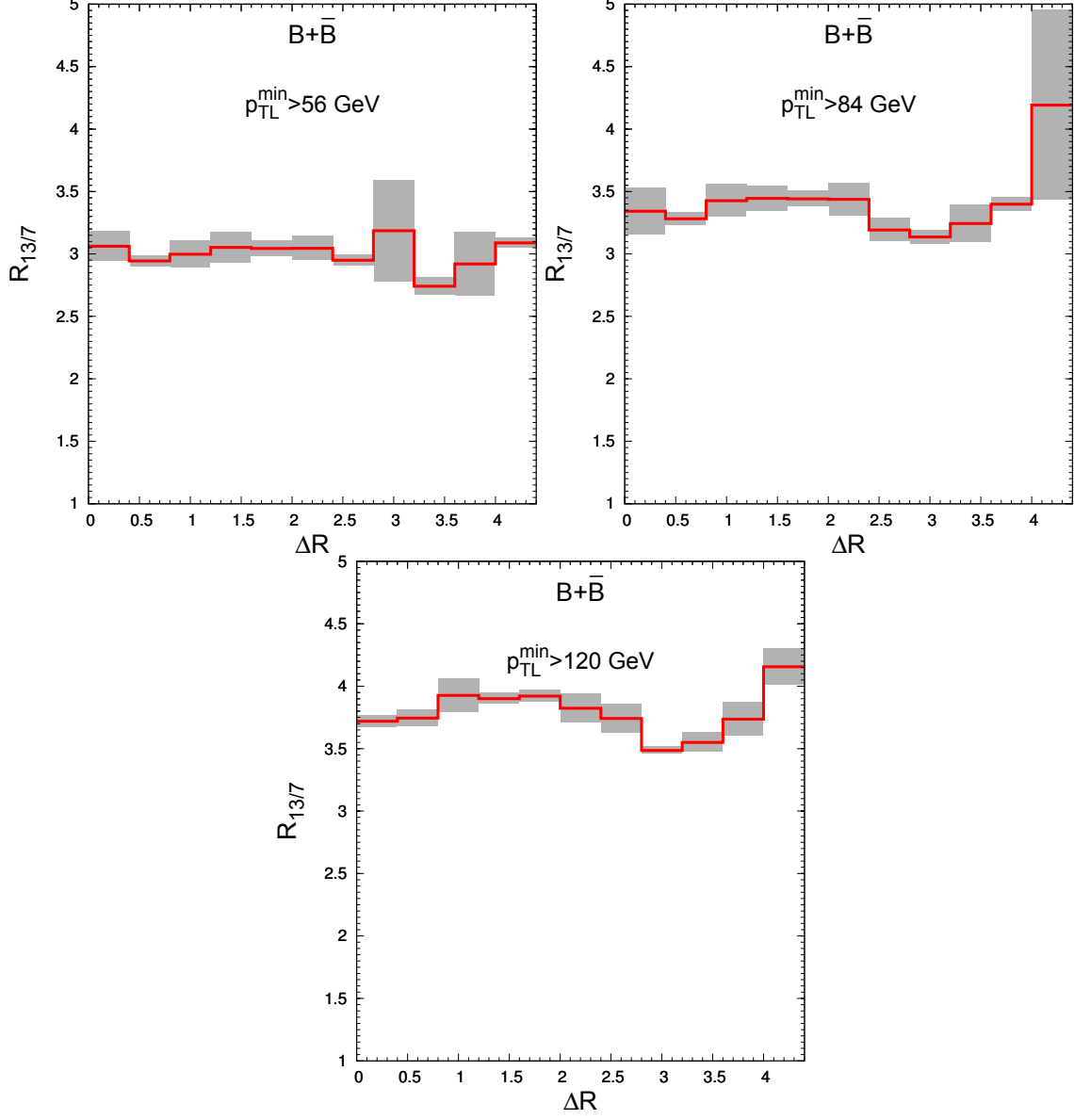


FIG. 12: Predictions for the ratio of $d\sigma/d\Delta R$ -spectra at $\sqrt{S} = 13 \text{ TeV}$ and $\sqrt{S} = 7 \text{ TeV}$ for the same kinematic cuts as in the Ref. [3].

-
- [1] CDF Collaboration, T. Aaltonen *et al.*, Measurement of the $b\bar{b}$ cross section using a dedicated trigger in $p\bar{p}$ collisions at 1.96 TeV. CDF note 8939, 2007, URL: <http://www-cdf.fnal.gov/physics/new/qcd/QCD.html>.
 - [2] ATLAS Collaboration, G. Aad *et al.*, G. Aad *et al.* [ATLAS Collaboration], “Measurement of the inclusive and dijet cross-sections of b^- jets in pp collisions at $\sqrt{s} = 7$ TeV with the ATLAS detector,” Eur. Phys. J. C **71**, 1846 (2011) doi:10.1140/epjc/s10052-011-1846-4 [arXiv:1109.6833 [hep-ex]].
 - [3] V. Khachatryan *et al.* [CMS Collaboration], “Measurement of $B\bar{B}$ Angular Correlations based on Secondary Vertex Reconstruction at $\sqrt{s} = 7$ TeV,” JHEP **1103**, 136 (2011) doi:10.1007/JHEP03(2011)136 [arXiv:1102.3194 [hep-ex]].
 - [4] R. Corke and T. Sjostrand, “Interleaved Parton Showers and Tuning Prospects,” JHEP **1103**, 032 (2011) doi:10.1007/JHEP03(2011)032 [arXiv:1011.1759 [hep-ph]].
 - [5] S. Frixione and B. R. Webber, “Matching NLO QCD computations and parton shower simulations,” JHEP **0206**, 029 (2002) doi:10.1088/1126-6708/2002/06/029 [hep-ph/0204244];
 - [6] S. Alioli, P. Nason, C. Oleari and E. Re, “A general framework for implementing NLO calculations in shower Monte Carlo programs: the POWHEG BOX,” JHEP **1006**, 043 (2010) doi:10.1007/JHEP06(2010)043 [arXiv:1002.2581 [hep-ph]].
 - [7] S. Catani, F. Krauss, R. Kuhn and B. R. Webber, “QCD matrix elements + parton showers,” JHEP **0111**, 063 (2001) doi:10.1088/1126-6708/2001/11/063 [hep-ph/0109231].
 - [8] H. Jung, M. Kraemer, A. V. Lipatov and N. P. Zotov, “Investigation of beauty production and parton shower effects at LHC,” Phys. Rev. D **85**, 034035 (2012) doi:10.1103/PhysRevD.85.034035 [arXiv:1111.1942 [hep-ph]].
 - [9] L. N. Lipatov, “Gauge invariant effective action for high-energy processes in QCD,” Nucl. Phys. B **452**, 369 (1995) doi:10.1016/0550-3213(95)00390-E [hep-ph/9502308].
 - [10] L. N. Lipatov and M. I. Vyazovsky, “QuasimultiRegge processes with a quark exchange in the t channel,” Nucl. Phys. B **597**, 399 (2001) doi:10.1016/S0550-3213(00)00709-4 [hep-ph/0009340].
 - [11] L. N. Lipatov, “Small x physics in perturbative QCD,” Phys. Rept. **286**, 131 (1997) doi:10.1016/S0370-1573(96)00045-2 [hep-ph/9610276].

- [12] E. N. Antonov, L. N. Lipatov, E. A. Kuraev and I. O. Cherednikov, “Feynman rules for effective Regge action,” Nucl. Phys. B **721**, 111 (2005) doi:10.1016/j.nuclphysb.2005.05.013, 10.1016/j.nuclphysb.2005.013 [hep-ph/0411185].
- [13] J. Bartels, L. N. Lipatov and G. P. Vacca, “Ward Identities for Amplitudes with Reggeized Gluons,” Phys. Rev. D **86**, 105045 (2012) doi:10.1103/PhysRevD.86.105045 [arXiv:1205.2530 [hep-th]].
- [14] J. R. Andersen, V. Del Duca and C. D. White, “Higgs Boson Production in Association with Multiple Hard Jets,” JHEP **0902**, 015 (2009) doi:10.1088/1126-6708/2009/02/015 [arXiv:0808.3696 [hep-ph]].
- [15] F. Hautmann, M. Hentschinski and H. Jung, “Forward Z-boson production and the unintegrated sea quark density,” Nucl. Phys. B **865**, 54 (2012) doi:10.1016/j.nuclphysb.2012.07.023 [arXiv:1205.1759 [hep-ph]].
- [16] M. Nefedov and V. Saleev, “Diphoton production at the Tevatron and the LHC in the NLO approximation of the parton Reggeization approach,” Phys. Rev. D **92**, no. 9, 094033 (2015) doi:10.1103/PhysRevD.92.094033 [arXiv:1505.01718 [hep-ph]].
- [17] A. Buckley *et al.*, “General-purpose event generators for LHC physics,” Phys. Rept. **504**, 145 (2011) doi:10.1016/j.physrep.2011.03.005 [arXiv:1101.2599 [hep-ph]].
- [18] M. A. Kimber, A. D. Martin and M. G. Ryskin, “Unintegrated parton distributions,” Phys. Rev. D **63**, 114027 (2001) doi:10.1103/PhysRevD.63.114027 [hep-ph/0101348].
- [19] A. D. Martin, M. G. Ryskin and G. Watt, “NLO prescription for unintegrated parton distributions,” Eur. Phys. J. C **66**, 163 (2010) doi:10.1140/epjc/s10052-010-1242-5 [arXiv:0909.5529 [hep-ph]].
- [20] M. A. Nefedov, V. A. Saleev and A. V. Shipilova, “Dijet azimuthal decorrelations at the LHC in the parton Reggeization approach,” Phys. Rev. D **87**, no. 9, 094030 (2013) doi:10.1103/PhysRevD.87.094030 [arXiv:1304.3549 [hep-ph]].
- [21] V. Saleev and A. Shipilova, “Inclusive b-jet and $b\bar{b}$ -dijet production at the LHC via Reggeized gluons,” Phys. Rev. D **86**, 034032 (2012) doi:10.1103/PhysRevD.86.034032 [arXiv:1201.4640 [hep-ph]].
- [22] R. Maciua, V. A. Saleev, A. V. Shipilova and A. Szczurek, “New mechanisms for double charmed meson production at the LHCb,” Phys. Lett. B **758**, 458 (2016) doi:10.1016/j.physletb.2016.05.052 [arXiv:1601.06981 [hep-ph]].

- [23] A. Karpishkov, V. Saleev and A. Shipilova, “Large- p_T production of D mesons at the LHCb in the parton Reggeization approach,” *Phys. Rev. D* **94**, no. 11, 114012 (2016) doi:10.1103/PhysRevD.94.114012 [arXiv:1610.04975 [hep-ph]].
- [24] A. V. Karpishkov, M. A. Nefedov, V. A. Saleev and A. V. Shipilova, “B-meson production in the Parton Reggeization Approach at Tevatron and the LHC,” *Int. J. Mod. Phys. A* **30**, no. 04n05, 1550023 (2015) doi:10.1142/S0217751X15500232 [arXiv:1411.7672 [hep-ph]].
- [25] B. A. Kniehl, M. A. Nefedov and V. A. Saleev, “Prompt-photon plus jet associated photo-production at HERA in the parton Reggeization approach,” *Phys. Rev. D* **89**, no. 11, 114016 (2014) doi:10.1103/PhysRevD.89.114016 [arXiv:1404.3513 [hep-ph]].
- [26] A. van Hameren and M. Serino, “BCFW recursion for TMD parton scattering,” *JHEP* **1507**, 010 (2015) doi:10.1007/JHEP07(2015)010 [arXiv:1504.00315 [hep-ph]]; K. Kutak, A. Hameren and M. Serino, “QCD amplitudes with 2 initial spacelike legs via generalised BCFW recursion,” *JHEP* **1702**, 009 (2017) doi:10.1007/JHEP02(2017)009 [arXiv:1611.04380 [hep-ph]].
- [27] A. van Hameren, “KaTie: for parton-level event generation with k_T -dependent initial states,” arXiv:1611.00680 [hep-ph].
- [28] A. D. Martin, W. J. Stirling, R. S. Thorne and G. Watt, “Parton distributions for the LHC,” *Eur. Phys. J. C* **63**, 189 (2009) doi:10.1140/epjc/s10052-009-1072-5 [arXiv:0901.0002 [hep-ph]].
- [29] B. A. Kniehl, G. Kramer, I. Schienbein and H. Spiesberger, *Phys. Rev. D* **77**, 014011 (2008) doi:10.1103/PhysRevD.77.014011 [arXiv:0705.4392 [hep-ph]].
- [30] M. Cacciari, G. P. Salam and G. Soyez, “The Anti- $k(t)$ jet clustering algorithm,” *JHEP* **0804**, 063 (2008) doi:10.1088/1126-6708/2008/04/063 [arXiv:0802.1189 [hep-ph]].
- [31] T. Hahn, “Generating Feynman diagrams and amplitudes with FeynArts 3,” *Comput. Phys. Commun.* **140**, 418 (2001) doi:10.1016/S0010-4655(01)00290-9 [hep-ph/0012260].
- [32] T. Hahn and M. Perez-Victoria, “Automatized one loop calculations in four-dimensions and D-dimensions,” *Comput. Phys. Commun.* **118**, 153 (1999) doi:10.1016/S0010-4655(98)00173-8 [hep-ph/9807565].
- [33] M. A. Nefedov, V. A. Saleev, *in preparation*.
- [34] T. Hahn, “CUBA: A Library for multidimensional numerical integration,” *Comput. Phys. Commun.* **168**, 78 (2005) doi:10.1016/j.cpc.2005.01.010 [hep-ph/0404043]; “Concurrent Cuba,” *J. Phys. Conf. Ser.* **608**, no. 1, 012066 (2015) doi:10.1088/1742-6596/608/1/012066 [arXiv:1408.6373 [physics.comp-ph]].

- [35] M. L. Mangano and J. Rojo, “Cross Section Ratios between different CM energies at the LHC: opportunities for precision measurements and BSM sensitivity,” JHEP **1208**, 010 (2012) doi:10.1007/JHEP08(2012)010 [arXiv:1206.3557 [hep-ph]].
- [36] D. Binosi and L. Theussl, “JaxoDraw: A Graphical user interface for drawing Feynman diagrams,” Comput. Phys. Commun. **161**, 76 (2004) doi:10.1016/j.cpc.2004.05.001 [hep-ph/0309015].